7. J. Faist, F. Capasso, C. Sirtori, D. L. Sivco, A. Y. Cho, in *Intersubband Transitions in Quantum Wells, Semiconductor and Semimetal*, H. C. Liu, F. Capasso, Eds. (Academic Press, London, 2000), vol. 66, chap. 1, and references therein.
8. Reciprocal space mapping along the (113) and (224) Bragg planes was performed.
9. T. Fromherz *et al.*, *Appl. Phys. Lett.* **68**, 3611 (1996).
10. T. Fromherz *et al.*, *Phys. Rev. B* **50**, 10573 (1994).
11. P. Kruck *et al.*, *Appl. Phys. Lett.* **76**, 3340 (2000).
12. J. Faist *et al.*, *Appl. Phys. Lett.* **63**, 1354 (1993).
13. J. Faist *et al.*, *Appl. Phys. Lett.* **65**, 94 (1994).
14. S. Blaser *et al.*, unpublished data.
15. P. Boucaud *et al.*, *Appl. Phys. Lett.* **69**, 3069 (1996).
16. In a recent sample we have also been able to demonstrate a confinement shift (observed EL energy, 154 meV; calculated HH2 → HH1 transition, 149 meV).

17. Supported by the Schweizerischer Nationalfonds and Bundesamt für Bildung und Wissenschaft Nr 99 0078. We thank M. Kummer, S. Blaser, D. Hofstetter, and S. Stutz for technical and analytical assistance.

14 September 2000; accepted 15 November 2000

Element-Selective Single Atom Imaging

K. Suenaga,[1,3]* M. Tencé,[1] C. Mory,[1] C. Colliex,[1,2] H. Kato,[4] T. Okazaki,[4] H. Shinohara,[4] K. Hirahara,[3] S. Bandow,[3] S. Iijima[3,5]

Electron energy-loss spectroscopy (EELS) is widely used to identify elemental compositions of materials studied by microscopy. We demonstrate that the sensitivity and spatial resolution of EELS can be extended to the single-atom limit. A chemical map for gadolinium (Gd) clearly reveals the distribution of Gd atoms inside a single chain of metallofullerene molecules (Gd@C_{82}) generated within a single-wall carbon nanotube. This characterization technique thus provides the "eyes" to see and identify individual atoms in nanostructures. It is likely to find broad application in nanoscale science and technology research.

Advances in nanotechnology increasingly rely on characterization tools with atomic resolution. Chemical information on heterogeneous nanostructures in particular is more and more crucial for diagnosing and predicting properties of nanodevices. Electron microscopies have long been able to image individual atoms (*1, 2*) but cannot be used to identify elements, because all scattered electrons are collected for imaging. For elemental identification of individual atoms in an electron microscope, only the inelastically scattered electrons that suffer element-specific energy loss must be counted. It has been predicted that the detection limit of EELS should be a single atom (*3*). However, convincing experimental evidence has been lacking because of the absence of fully adapted test objects (*4*).

Here, we demonstrate single-atom spectroscopy by means of EELS. For this purpose, a perfectly suited specimen exhibiting a sequence of individual atoms positioned at regular intervals has been selected. It is found in a recently synthesized hybrid nanomaterial, a single-walled carbon nanotube (SWNT) encapsulating a chain of metallofullerenes (*5*). A scanning transmission electron microscope (VG HB501) that provides a tiny electron beam with a high current flux (~650 pA in a probe 0.5 to 0.6 nm in diameter) and a high-efficiency charge-coupled device–based detector after an electron spectrometer (modified Gatan PEELS 666) were used for the experiment. The focused incident probe can scan the object under investigation with accurate step increments on the order of angstroms, allowing a whole EELS spectrum to be recorded within a few milliseconds at each probe position. Hence, the intensity of characteristic energy-loss edges can be derived with highly accurate spatial information, and consequently the mapping of the searched element is feasible (*6*).

A chain of endohedral Gd-metallofullerenes was recently generated inside a SWNT by this research group (*5*). Such a material is ideal for demonstrating single-atom spectroscopy, because this structure involves isolated Gd atoms separated by 1 to 2 nm (Fig. 1). The metallofullerene molecules (Gd@C_{82}) are aligned within a SWNT. The dark spots seen on each fullerene structure in the high-resolution image are suspected to be the encapsulated Gd atoms (*7*). The interval between the adjacent Gd atoms is large enough with respect to the smallest probe size (~0.5 nm) accessible with our current electron optics. Element-selective imaging has been performed on a structure similar to that in Fig. 1. A set of 128×32 spectra was recorded with a 3 Å step (consequently, the scanned area corresponds to ~40×10 nm). Each spectrum was acquired in as little as 35 ms with enough counting statistics. Intensities of the Gd N_{45} edge and carbon K edge were extracted pixel per pixel from all the individual spectra (*8*), and chemical maps for both elements were constructed (Fig. 2).

The bright spots in Fig. 2A are aligned along the nanotube direction, which indicates that they correspond to the Gd atoms. Comparison with the simultaneously obtained carbon map (Fig. 2B) shows that the Gd atoms are located inside the carbon nanotube. This is further confirmed in Fig. 2C, which displays the Gd map (smoothed by convolution with a 3×3 pixel matrix) superposed on the carbon map. Therefore, we can confirm that doping the carbon nanotubes with metallofullerenes has been successful and that the dark spots seen in the high-resolution image (Fig. 1) explicitly correspond to the Gd atoms.

The arrows in Fig. 2B indicate the approximate positions of the individual Gd atoms. The interval between them is about 1 to 3 nm, and some of the Gd atoms are missing. This is probably because the Gd atoms tend to move around from the original positions and, under the intense electron beam, make an aggregate of one to three (or four) atoms associated with a fusion of the adjacent metallofullerenes. Such coalescence processes between the metallofullerenes under the electron beam have also been observed in situ during high-resolution electron microscopy observations. Note that our present spatial resolution (~0.5 nm) is not sufficient to resolve the carbon layer spacing (~0.34 nm) between the adjacent fullerenes and nano-

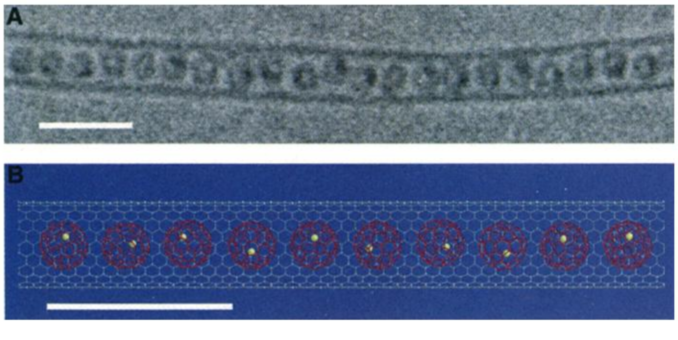

Fig. 1. A conventional high-resolution image (**A**) and a schematic presentation (**B**) of a similar structure. A chain of endohedral Gd-metallofullerenes (Gd@C_{82}) is encapsulated in a SWNT. The Gd atoms are shown in yellow in (**B**). Scale bars, 3 nm.

---

[1]Laboratoire de Physique des Solides (CNRS UMR 8502), [2]Laboratoire Aimé Cotton (CNRS UPR 3321), Université Paris-Sud, Orsay 91405, France. [3]Japan Science and Technology Corporation, "Nanotubulites" project, Meijo University, Nagoya 468-8502, Japan. [4]Department of Chemistry, Nagoya University, Nagoya 464-8602, Japan. [5]NEC Corporation, Tsukuba 305-8501, Japan.

*To whom correspondence should be addressed. E-mail: suenaga@meijo-u.ac.jp

tube, but can resolve the adjacent Gd atoms in this specific experiment.

A typical single EELS spectrum (Fig. 3) located at the apex of a Gd atom image shows the energy windows used for calculating the respective intensities in the elemental maps. The spectrum ensures that the weight of the Gd N edge (~140 eV) is notably higher than the noise level. To quantify the number of Gd atoms, we scaled the background-stripped weight of the Gd N edge (140 to 155 eV) at a given pixel to the total number of counts in the corresponding spectrum (estimated from the probe current and the detector efficiency) using the suitable cross section calculated with the Hartree-Slater model and convergence angle corrections. Because the examined specimen is extremely thin with respect to the inelastic mean free path for electron transmission, no multiple scattering effect (thickness effect) needs to be considered for the quantification. The number of atoms involved in a single EELS spectrum should therefore be

$$N_{\text{atom}} = (I/I_0)\cdot(1/\sigma)\cdot A \tag{1}$$

where I and I_0 are the measured counts for the edge and the total counts for the whole spectrum, respectively, σ is the cross section for the edge, and A is the probed area (*9*).

Table 1 summarizes the consequent quantification result for the number of involved Gd atoms at each of the points indicated by arrows in Fig. 2A. The numbers of identified atoms are not exact integers and have some ambiguity because, during the recording of one spectrum, the individual atoms may move within their fullerene cages and spend only a fraction of the measurement time within the incident electron beam section. Also, there is uncertainty in the cross section used for the normalization and the estimated probed area (*10*). This result clearly shows that some of the Gd atoms have migrated from their original positions to travel along the nanotube and form the three- or four-atom clusters under investigation, and it therefore reflects the inherent experimental difficulties: The intense electron beam necessary to extract a single-atom spectrum disrupts this type of specimen structure (*11*). Despite these difficulties, this study unambiguously demonstrates that element-specific single-atom detection is possible by EELS (at positions a, b, g, h, and i in Fig. 2A). This has been made possible by the use of the image-spectrum mode for acquiring large numbers of spectra (4096 spectra in the present case) over an extended area including the objects of interest. Processing all these spectra individually gives access to statistical distributions of counts as a function of pixel position, and constitutes a hint for evaluating the signal-to-noise ratio (SNR) in the measurements and the ultimate sensitivity of the technique.

This technique is able to distinguish atoms even with only one atomic number difference. However, its applicability is not universal, because for some elements the characteristic core edges are of poor contrast and/or low intensities (i.e., for noble metals). It is mostly suited for the identification of low–atomic number elements, transition metals, lanthanides, and uranides. Possible applications of this technique include selective labeling of active sites on biomolecules.

Moreover, the Gd M_{45} edge (~1217 eV) can yield more information than the N edge about the valence state and the spin state of the encapsulated Gd atom (*12*). The M edge analysis would therefore enable us to obtain the electronic and magnetic information from

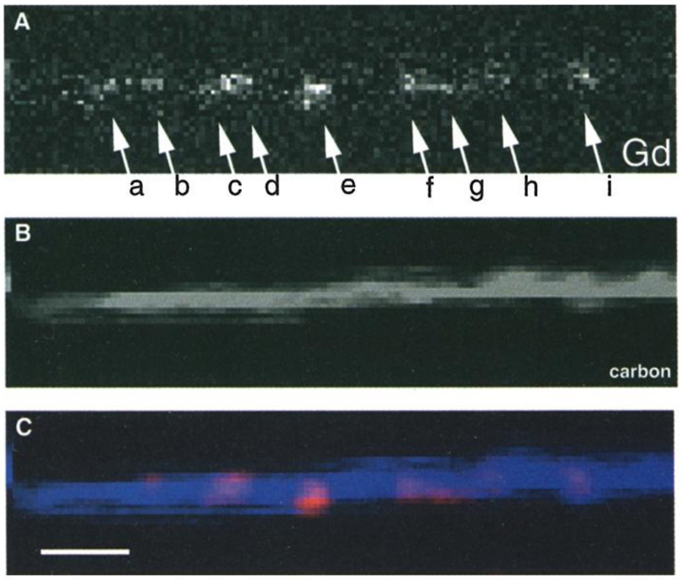

Fig. 2. Element-selective images for gadolinium (**A**) and carbon (**B**) and a constructed color image (Gd, red; carbon, blue) (**C**). The Gd atoms are clearly identified within the carbon nanotube and distributed along the nanotube axis. Scale bar, 3 nm.

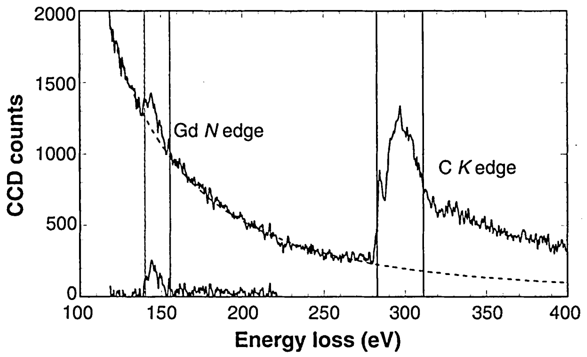

Fig. 3. A typical EELS spectrum acquired within 35 ms, showing the Gd N edge and carbon K edge (chosen at the central pixel of a Gd atom). The background stripped Gd N edge is crucial with respect to the noise level and implies that one (or two) Gd atom(s) are involved. From the corresponding values for the signal (~4000 counts) and for the background (~30,000 counts), one can estimate that the SNR for single-atom identification in this experiment is higher than 3, which corresponds to a 98% confidence level for detection.

Table 1. Quantification results for the number of Gd atoms involved at each spectrum point indicated by arrows in Fig. 2A. The values for I correspond to characteristic Gd signal (after background subtraction) measured at the pixel position with highest count rate. The numbers involved in the corresponding estimation of N_{atom} are deduced from Eq. 1 incorporating the numerical values summarized in (*10*). The practical error level in this experiment, estimated from the sources of inaccuracy on the different parameters involved in Eq. 1, is typically one atom (*13*). This analysis demonstrates that some of the Gd atoms have migrated within a SWNT to produce three- or four-atom clusters as a result of the beam-induced specimen modifications. The number of Gd atoms that have migrated from their original positions (marked "0") to form clusters of a few atoms corresponds to the number of absent metallofullerenes estimated from the distance between the arrows.

Point	I	N_{atom}
a	4,400	1
b	4,291	1
	490	0
c+d	10,932	3 or 4
	761	0
	222	0
e	13,990	4 or 3
	148	0
	187	0
f	4,567	2 or 1
g	3,396	1
h	3,999	1
	1,907	0 or 1
i	4,157	1

the single atom. In the current experimental condition, however, the single-atom counting statistics for the M edge are barely sufficient for recording, because its cross section is a fraction of that of the N edge. More sophisticated electron optics for the microscope and more efficient detectors with lower noise are required for a practical use of this approach.

References and Notes

1. A. V. Crewe *et al.*, *Science* **168**, 1338 (1970).
2. S. Iijima, *Optik* **47**, 437 (1977).
3. M. Isaacson, D. Johnson, *Ultramicroscopy* **1**, 33 (1975).
4. O. L. Krivanek, C. Mory, M. Tence, C. Colliex, *Microsc. Microanal. Microstruct.* **2**, 257 (1991).
5. K. Hirahara *et al.*, *Phys. Rev. Lett.*, in press. The starting material ($Gd@C_{82}$) has been purified (99.9% up) by multistage high-performance liquid chromatography.
6. C. Colliex *et al.*, *J. Electron Microsc.* **48**, 995 (1999).
7. The high-resolution image was taken by a conventional transmission electron microscope (JEOL 2010F). The image agrees well with a simulated image [N. Tanaka, Y. Honda, M. Kawahara, M. Kishida, H. Shinohara, *Thin Solid Films* **281–282**, 613 (1996)].
8. R. F. Egerton, *EELS in the Electron Microscope* (Plenum, New York, ed. 2, 1996), pp. 245–300.
9. C. Mory, C. Colliex, *Ultramicroscopy* **28**, 339 (1989).
10. In this experiment, the values are estimated as A = 0.2 to 0.3 nm^2, $\sigma = 8.7 \times 10^{-7}$ nm^2, and $I_0 = 8 \times 10^8$ to 16×10^8. The inaccuracy for the quantified number of atoms is within 1.
11. This also explains why some of the Gd atoms are missing in Fig. 2A. Because the Gd atoms have migrated to move out from the viewed area, the total number of atoms detected is apparently less than the number expected.
12. K. Suenaga, S. Iijima, H. Kato, H. Shinohara, *Phys. Rev. B* **62**, 1627 (2000).
13. Further processing, relying on measurements after convolution with a (3 × 3) matrix, provides more reliable data with reduced sensitivity to noise fluctuations. They demonstrate that for point a, the number of atoms would more likely be 0 or 1, whereas for point i, it would more likely correspond to 2.
14. Supported in part by an international cooperative research project on "Nanotubulites" established between the Japan Science and Technology Corporation and CNRS. The Japan Society for the Promotion of Science Research for the Future Program on New Carbon Nano-Materials is also acknowledged by H.S. We thank one referee for his extended analysis of the displayed data and positive suggestions.

16 August 2000; accepted 24 October 2000

A Quantum Dot Single-Photon Turnstile Device

P. Michler,[1]* A. Kiraz,[1] C. Becher,[1] W. V. Schoenfeld,[2]
P. M. Petroff,[1,2] Lidong Zhang,[1] E. Hu,[1,2] A. Imamoğlu[1,3,4]†

Quantum communication relies on the availability of light pulses with strong quantum correlations among photons. An example of such an optical source is a single-photon pulse with a vanishing probability for detecting two or more photons. Using pulsed laser excitation of a single quantum dot, a single-photon turnstile device that generates a train of single-photon pulses was demonstrated. For a spectrally isolated quantum dot, nearly 100% of the excitation pulses lead to emission of a single photon, yielding an ideal single-photon source.

Conventional sources of light, such as light-emitting diodes and lasers, generate radiation that can be successfully described with classical Maxwell's equations. On the other hand, several applications in the emerging field of quantum information science require weak optical sources with strong quantum correlations between single photons (*1*). This is particularly true for quantum cryptography, which exploits the fundamental principles of quantum mechanics to provide unconditional security for communication. An essential element of secure key distribution in quantum cryptography is an optical source emitting a train of pulses that contain one and only one photon (*2*). Because measurements unavoidably modify the state of a single quantum system, an eavesdropper cannot gather information about the secret key without being noticed, provided that the pulses used in transmission do not contain two or more photons. More recently, it has also been shown that the availability of a single-photon source enables implemention of quantum computation using only linear optical elements and photodetectors (*3*). Here we report the experimental demonstration of an ideal single-photon source, which uses the anharmonicity of single quantum dot (QD) multiexciton transitions to regulate the photon generation process. Realization of such a source, termed a single-photon turnstile device (*4*), has been one of the holy grails of quantum electronics research, because it represents the ultimate limit in the quantum control of the photon generation process.

It is known that a driven single anharmonic quantum system, such as an atom or a molecule, exhibits photon antibunching; that is, a dead time between successive photon emission events (*5*). With the use of Hanbury-Brown and Twiss (HBT)–type photon correlation measurements (*6*), photon antibunching has been observed in a variety of single quantum emitters, for example, an atom (*7*), a stored ion (*8*), a molecule (*9*), a semiconductor QD (*10*, *11*), and a single nitrogen-vacancy center in diamond (*12*, *13*). Photon antibunching is a necessary but not sufficient condition for a single-photon turnstile device; an additional mechanism for regulating the excitation process is required to realize single-photon pulses.

A single-photon turnstile device based on a mesoscopic double-barrier p-n heterojunction was proposed in 1994 (*4*). An extension of this proposal was recently demonstrated (*14*), in which single as well as multiple photon emission events with a repetition rate of 10 MHz at 50 mK were reported. This device uses Coulomb blockade of tunneling for electrons and holes in a mesoscopic p-n diode structure to regulate the photon generation process. In this scheme, single-electron and hole-charging energies must be large compared to the thermal background energy to ensure single-photon emission. Therefore, this device can only be operated at ultra-low temperatures ($T \leq 1$ K). A triggered single-photon source based on a single molecule has been demonstrated (*15*) whereby regulation of the photon emission process is achieved by combining adiabatic passage techniques with pulsed optical excitation. With the use of photon correlation measurements, it was concluded that approximately 74% of the pulses give rise to single-photon emission at 1.8 K, with a repetition rate of a few megahertz.

The single-photon source that we report is based on a single QD embedded in a high-quality factor (Q) microcavity structure (*16*). The distinguishing feature of our QD single-photon source is the absence of pulses that contain more than one photon. To ensure single-photon generation at the fundamental QD exciton transition (1X), we adjust the pump power so that two or more electron-hole pairs are captured by the QD during each excitation pulse. The energy of the photons emitted during relaxation depends significantly on the number of multiexcitons that exist in the QD, due to Coulomb interactions enhanced by strong carrier confinement (*16*). If the total recombination time of the multiexciton QD state is longer than the recombination time of the free electron-hole pairs, each excitation pulse can lead to at most one photon emission event at the 1X transition. Therefore, regulation of the photon emission process can be achieved because of a combi-

---

[1]Department of Electrical and Computer Engineering, [2]Materials Department, [3]Department of Physics, University of California, Santa Barbara, CA 93106, USA. [4]Sabanci University, Orhanli 81474 Tuzla, Istanbul, Turkey.

*Present address: Institut für Festkörperphysik, Universität Bremen, Post Office Box 330440, D-28334 Bremen, Germany.

†To whom correspondence should be addressed. E-mail: atac@ece.ucsb.edu